Basics

on

Collider Physics

Outline

1. Collider Basics
2. Overview of a collider detector
3. CMS detector
4. A calculation of cross section, Drell-Yan, Z'
5. Kinematics, e.g., in Higgs boson search.

1. Collider Basics

In a collider experiment one measures the number of events for the signal

$$N_{\rm observed} = \sigma_{\rm process} \times \epsilon_{\rm detection} \times \int \mathcal{L} dt \;\; + \;\; N_{\rm bkgd}$$

$\sigma_{\rm process} \equiv$ cross section of the signal process, e.g., your Higgs boson, extra dimension signal that one wants to look at.

$\epsilon_{\rm detection} \equiv$ probability that the signal to be observed in the detector, including detector coverage, cut efficiencies, detector efficiencies.

$\int \mathcal{L} dt \equiv$ integrated luminosity.

$N_{\rm bkgd} \equiv$ no. of bkgd events that will go into the detector under the same selection cuts.

Goals:

- To search for something that are searchable: large enough $\sigma_{\rm process}$,
- To minimize $N_{\rm bkgd}$,
- To maximize $\epsilon_{\rm detection}$.

To calibrate the luminosity $\mathcal{L}$ is as important as the others

$$\mathcal{L} = f\,\frac{N_p N_{\bar p}}{4\pi\sigma_x\sigma_y}$$

where f: the freq. that beam bunches cross (1.7 MHz at the Tevatron), $N_{p,\bar p}$: no. of protons/bunch, $\sigma_{x,y}$ are sizes of the beam.

Typical beam size at hadron colliders are $20-100\mu$m, and $\mathcal{L} \sim 5\times 10^{31}$ cm^{-2} s^{-1}. Integrated luminosity $\int \mathcal{L} dt$ is usually given in pb^{-1} (1 pb$^{-1} = 10^{36}$ cm^{-2}).

During a typical week, Tevatron can accumulate $O(10)$ pb^{-1}. A cross section of 0.1 pb will give about one event per week.

2. Overview of a Particle Detector

The design of a particle detector depends on

- physics goals: what is it built for?
- cost

Basic components:

- Tracking system: a tracking volume with a high $\vec{B}$ field to measure the trajectory of charged particles with high precision. It is usually has an inner high resolution unit built with silicon to detect decays of short-lived particles. And an outer tracker with less expensive materials optimized momentum measurements.
- Calorimetry: made up of heavy material to absorb and detect all strongly and EM interacting particles. EM calorimeter (ECAL) and hadronic calorimeter (HCAL).
- Muon system: stop and measure the muon energy.
- Trigger system: complex systems of fast electronics and computers .

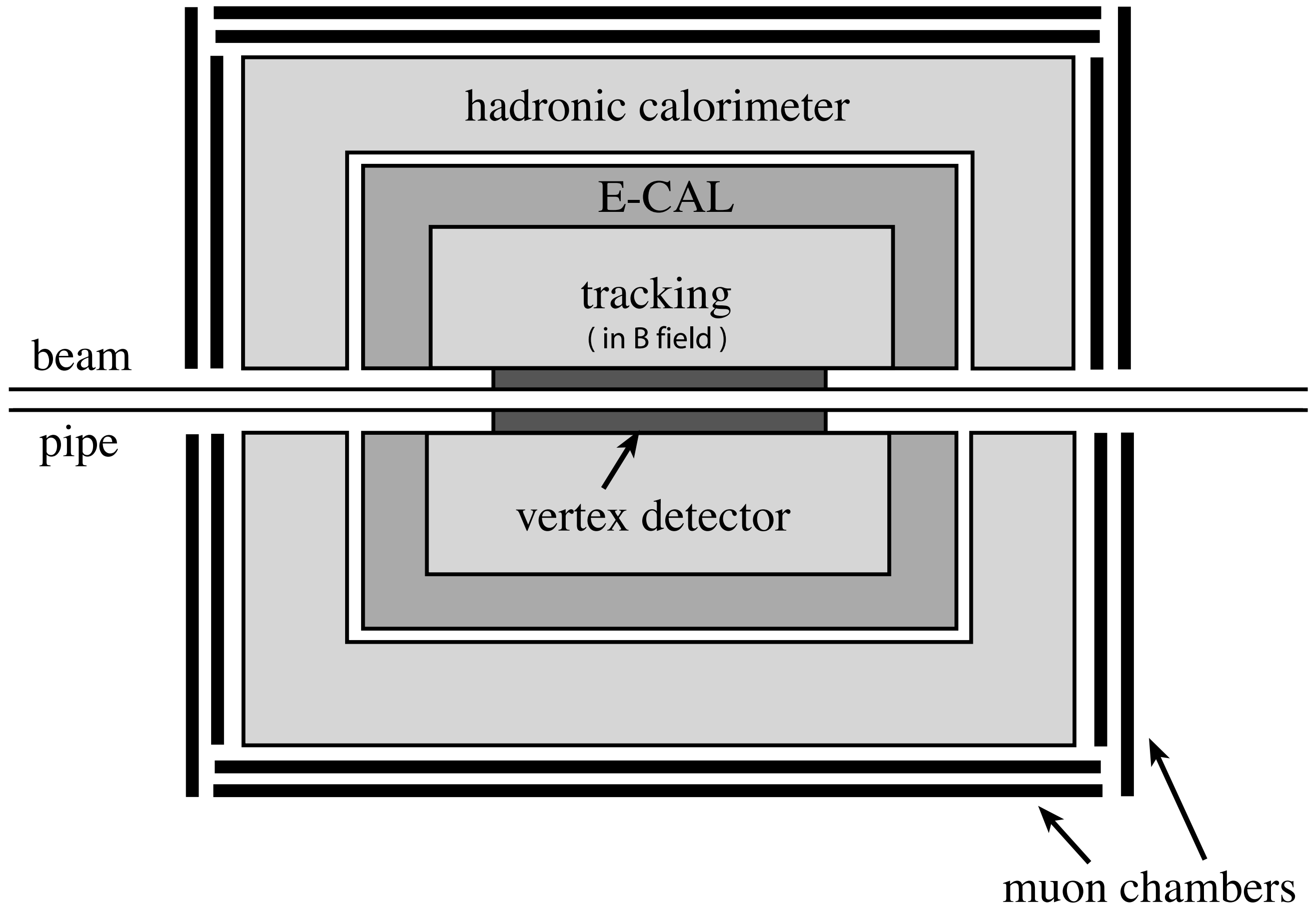
hadronic calorimeter
E-CAL
tracking
(in B field)
beam
pipe
vertex detector
muon chambers

Han

DØ Detector

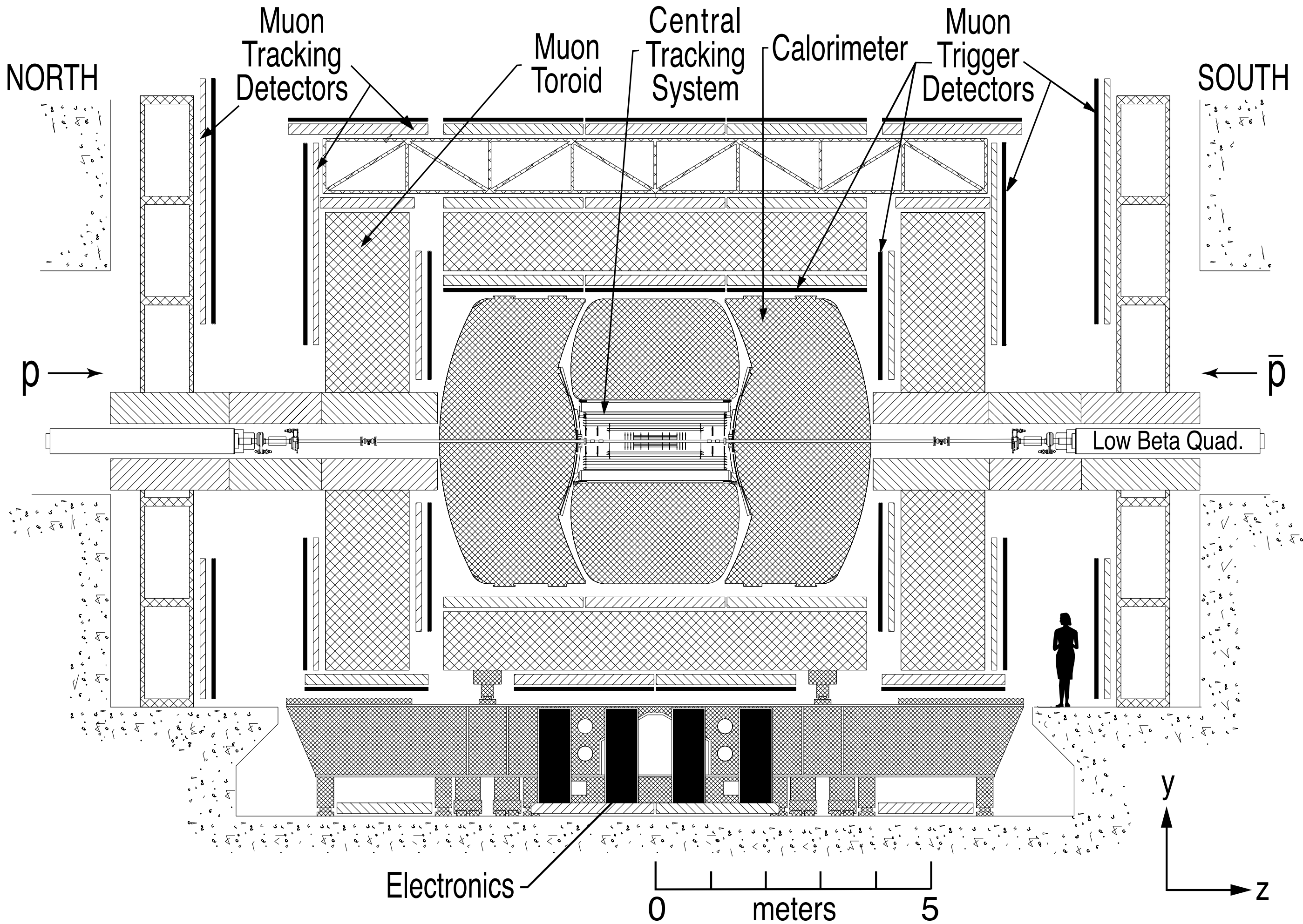

Muon Tracking Detectors
Muon Toroid
Central Tracking System
Calorimeter
Muon Trigger Detectors
NORTH
SOUTH
p
p̄
Low Beta Quad.
Electronics
0
meters
5
y
z

How are particles detected in the detector

Most particles will decay right after they are produced, e.g., W, Z, H, Z', RS graviton, ... We do not see them directly.

Colored particles (q, g) will hadronize into hadrons, such as $\pi, K, p, n, \ldots$

The distance that a particle travels in the detector

$$d = \gamma c \tau = (300\ \mu\mathrm{m}) \left(\frac{\tau}{10^{-12}\ \mathrm{s}} \right) \gamma$$

- Short-lived particles decay instantaneously into other particles, such as π^0, ρ.
- Particles with displaced vertex has a $\tau \sim 10^{-12}$ s, such as B, D, $\tau^\pm$.
- Quasi-stable particles with $\tau \gtrsim 10^{-10}$ s will interact with the detector before decay.
- Particles that do not interact with the detector at all, leading to missing transverse energy.

So at the end, the detector will only "see" γ, $e^\pm$, $\mu^\pm$, $\pi^\pm$, K, p, n.

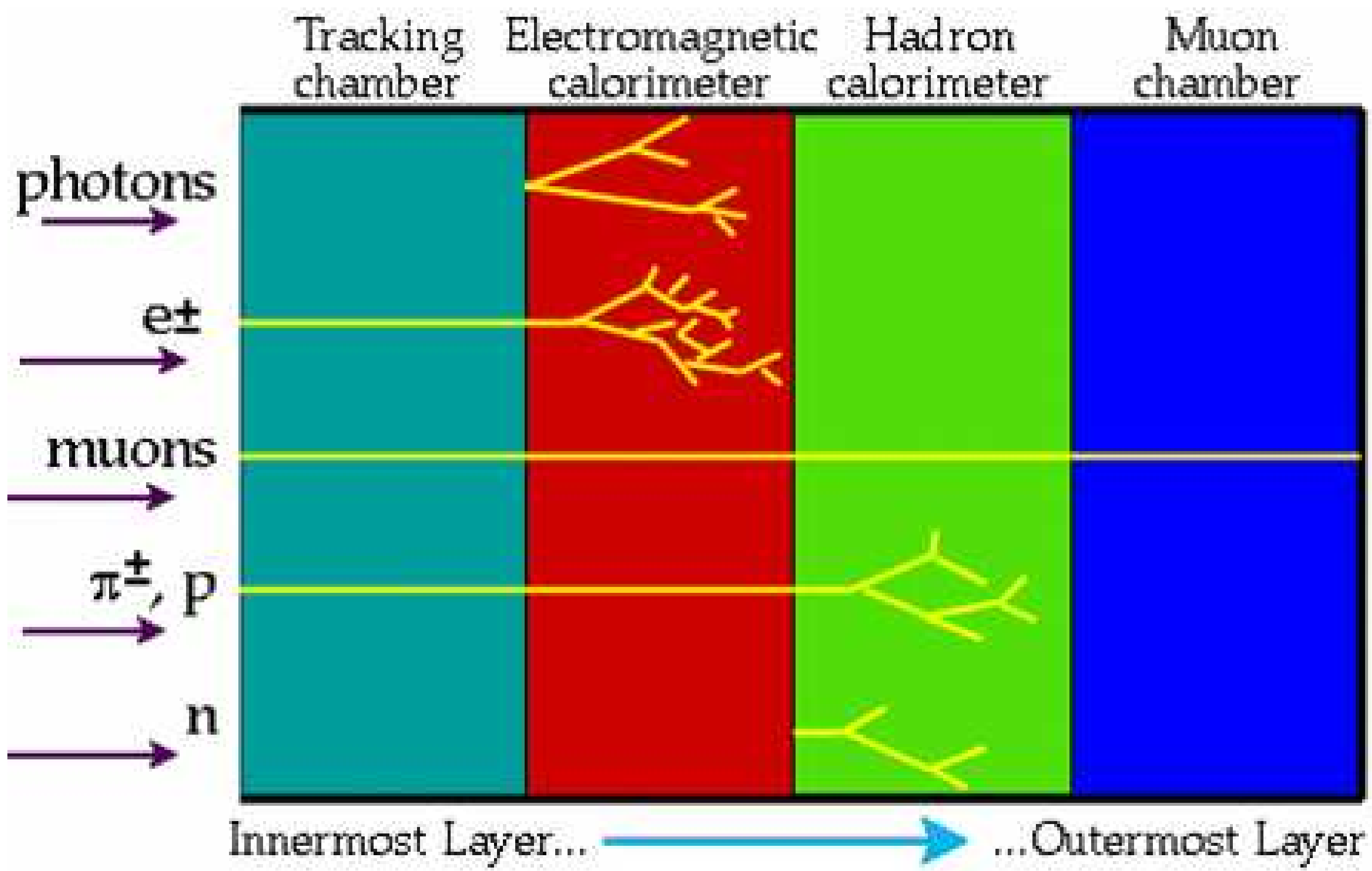
Tracking chamber
Electromagnetic calorimeter
Hadron calorimeter
Muon chamber
photons
e±
muons
π±, p
n
Innermost Layer...
...Outermost Layer

Han

3. Compact Muon Solenoid (CMS) Detector

- Silicon tracking system
- Preshower
- ECAL
- HCAL
- Forward calorimeter
- Muon chambers
- Superconducting magnets

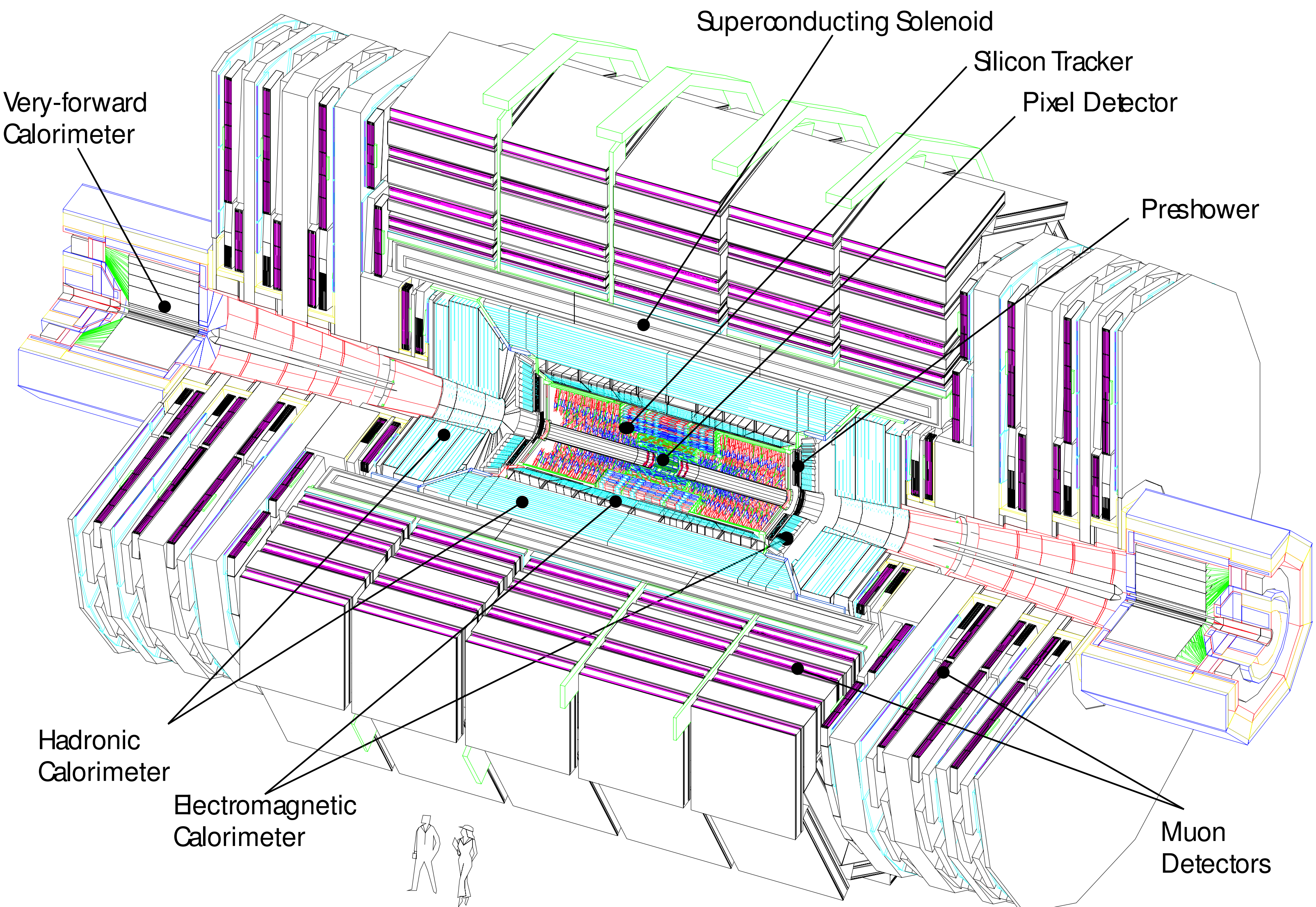

Compact Muon Solenoid

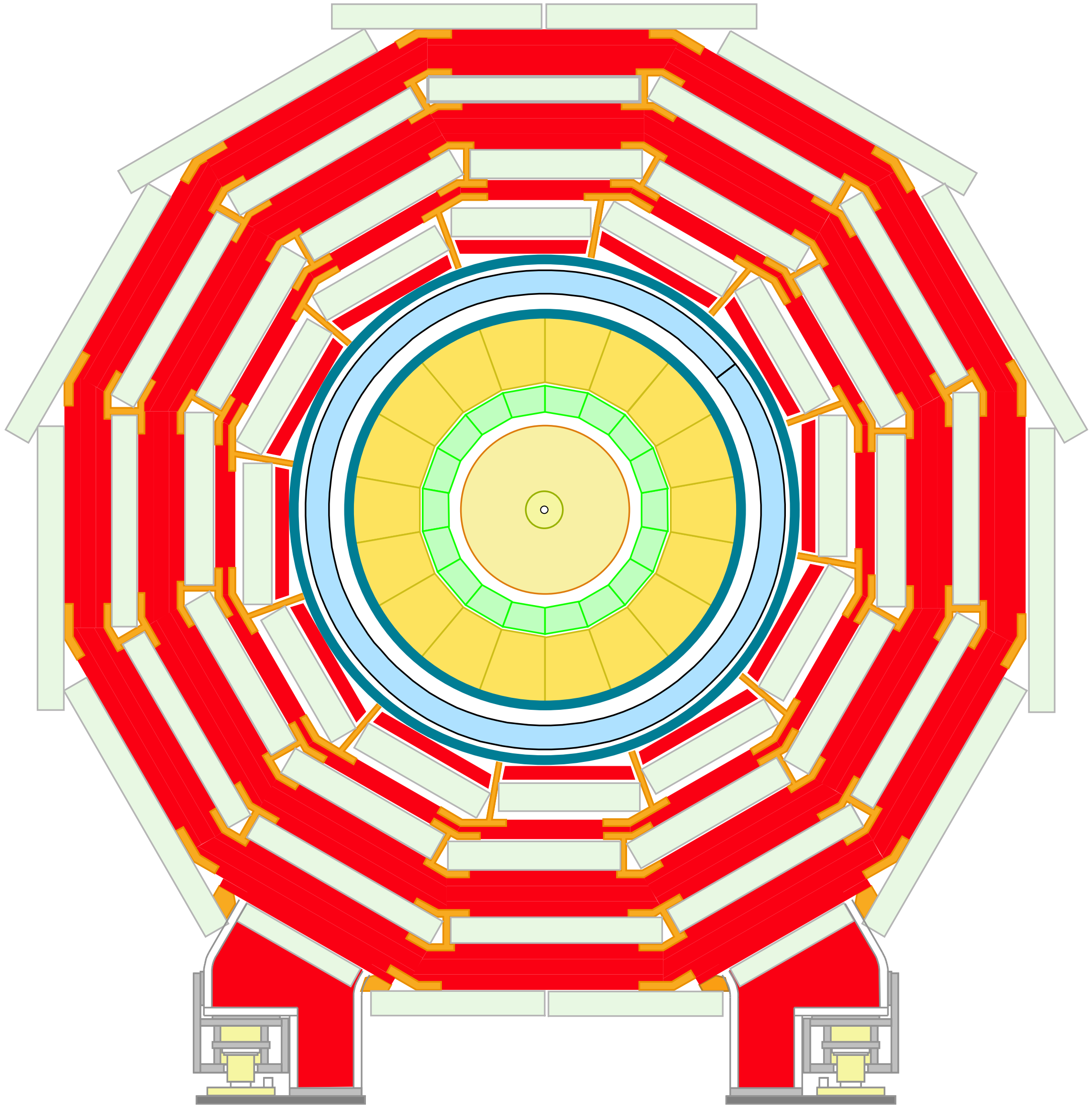

3.1 Tracking System

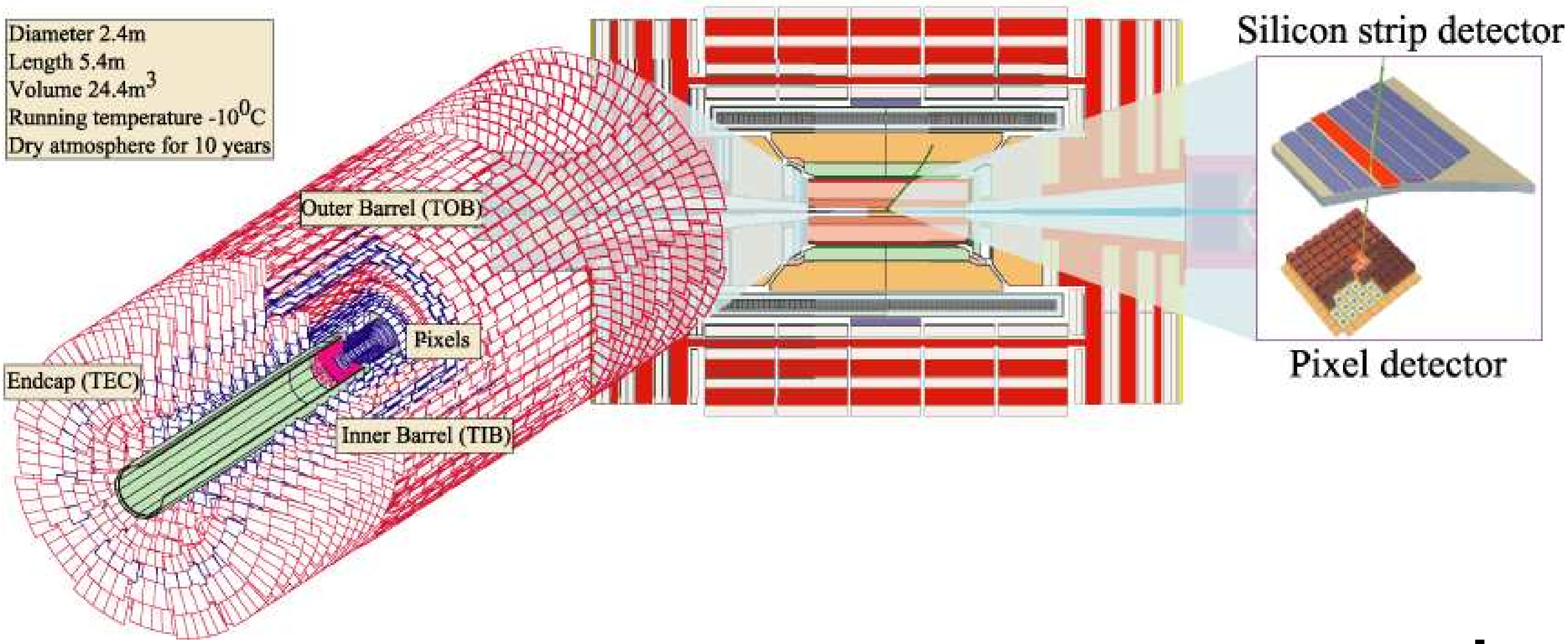

Tracking system is designed to reconstruct high-p_T $\mu^\pm$, isolated $e^\pm$ and charged hadrons with high momentum resolution and $\epsilon > 98\%$ in the range $|\eta| < 2.5$.

It is also designed to allow the identification of tracks coming from detached vertices (displaced vertices).

Two detector technologies are employed, each best matched to satisfying the stringent resolution, granularity and robustness requirements in the high (silicon pixels) medium and low occupancy (silicon microstrips) regions.

Momentum Measurements

Reconstructing the trajectory yields radius of curvature R. The particle's transverse momentum $p_T \perp \vec{B}$ can be determined

$$p_T \propto q\ B\ R$$

Resolution is

$$\frac{\delta p_T}{p_T} = (15 p_T + 0.5)\% \ \longrightarrow\ (60 p_T + 0.5)\%$$

for $|\eta| < 1.6$ to $|\eta| < 2.5$, and p_T in TeV.

For muons, by combining with the outer muon chamber the momentum resolution is better than 10% even at 4 TeV.

The CMS design is based on a superconducting solenoid providing a very high (4T) magnetic field.

Displaced Vertex

The ability to reconstruct the decay vertices of long-lived particles is crucial for numerous physics analyses. E.g. B-tagging.

At least 2 charged tracks are needed to reconstruct a secondary vertex:

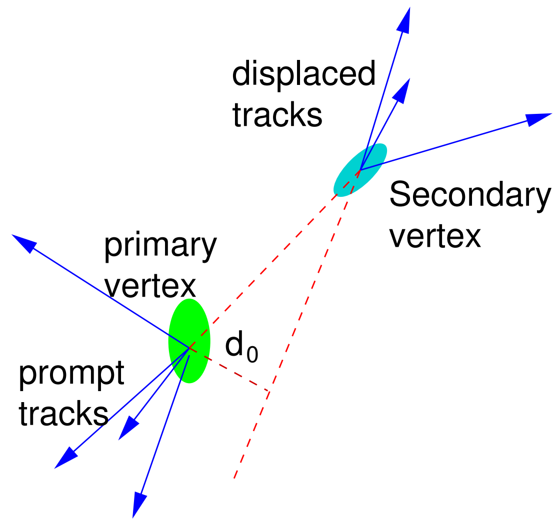

The impact parameter d_0 determines the displaced vertex. The resolution can be as small as $O(10)$ μm for $p_T \sim 100$ GeV, thanks to the pixel detector.

The position of such vertices depends on the lifetime of the particle, e.g., K_s a few cm, B mesons $1-2$ mm.

3.2 Calorimetry: Preshower, ECAL, HCAL

Electrons, photons and hadrons (p, n) are stopped by the calorimeters allowing their energy to be measured. Charged particles lose energy primarily by ionization, given by

Bethe-Bloch eq:

$$-\frac{dE}{dx} \propto \left(\frac{Q}{\beta}\right)^2$$

The first calorimeter layer is designed to measure the energies of electrons and photons with high precision. Since these particles interact electromagnetically, it is called an electromagnetic calorimeter (ECAL).

The Preshower has two-shower separation capability to reject $\pi^0 \to \gamma\gamma$, which is a serious background for $h \to \gamma\gamma$ decay.

Particles that interact via the strong interaction, hadrons, deposit most of their energy in the next layer, the hadronic calorimeter (HCAL).

ECAL

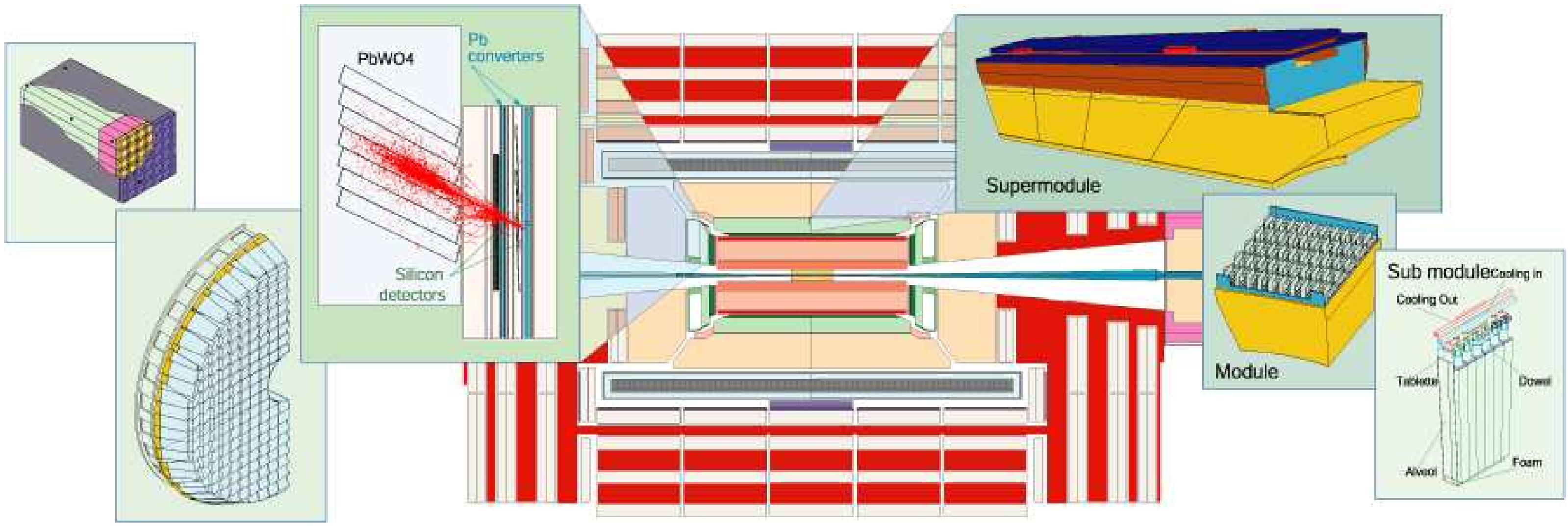

A scintillating crystal calorimeter offers excellent performance for energy resolution since almost all of the energy of electrons and photons is deposited within the crystal volume. CMS has chosen lead tungstate crystals which have high density, a small Moliere radius and a short radiation length allowing for a very compact calorimeter system. A high-resolution crystal calorimeter enhances the $H \to \gamma\gamma$ discovery.

The preshower detector contains two thin lead converters followed by silicon strip detector planes placed in front of the ECAL. The fine granularity of the detector enables the separation of single showers from overlaps of two close showers due to the photons from π^0 decays.

The expected signal from the decay $H \to \gamma\gamma$ for $M_H = 130$ GeV after 100 fb^{-1} collected at high luminosity.

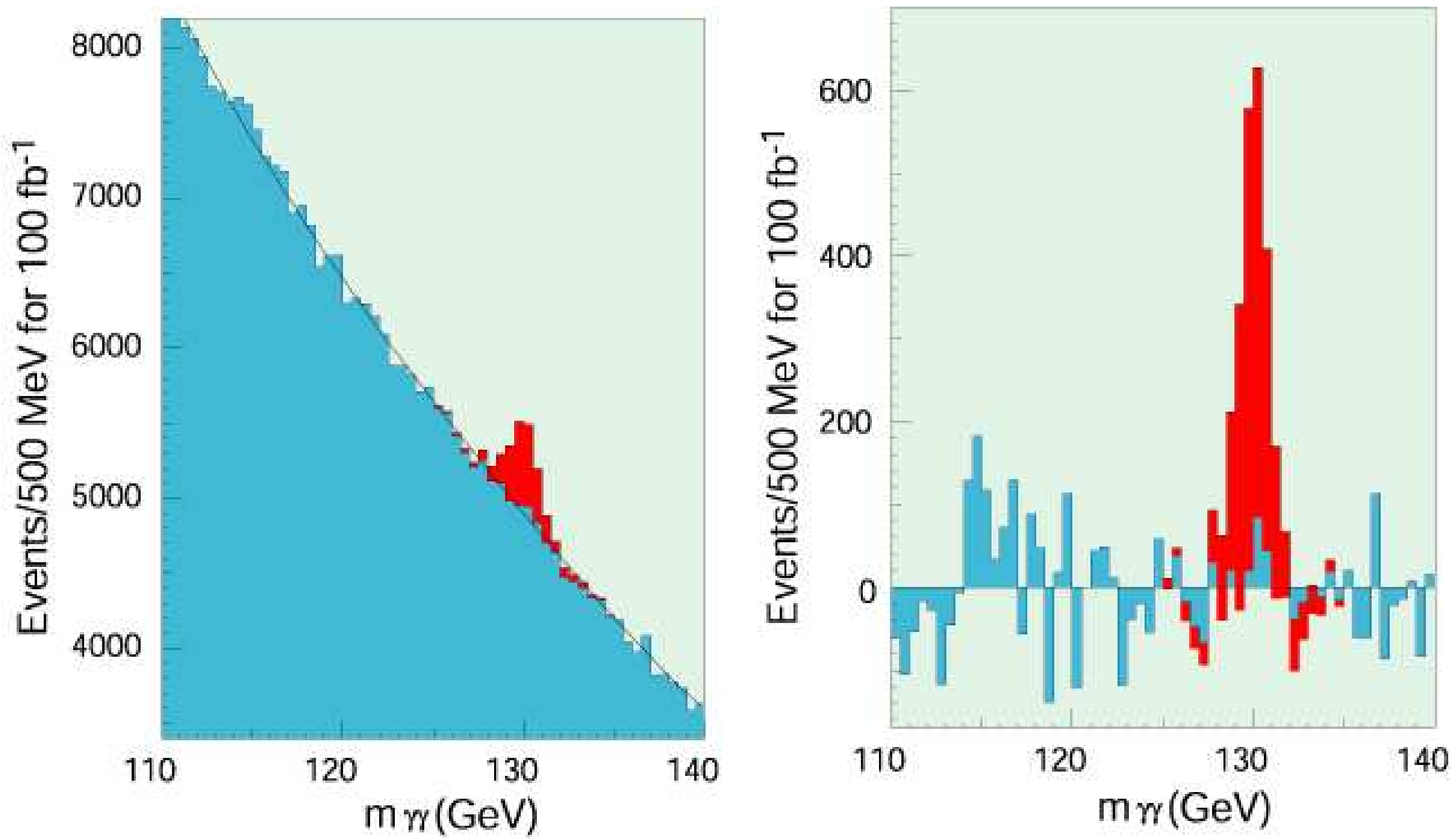

HCAL

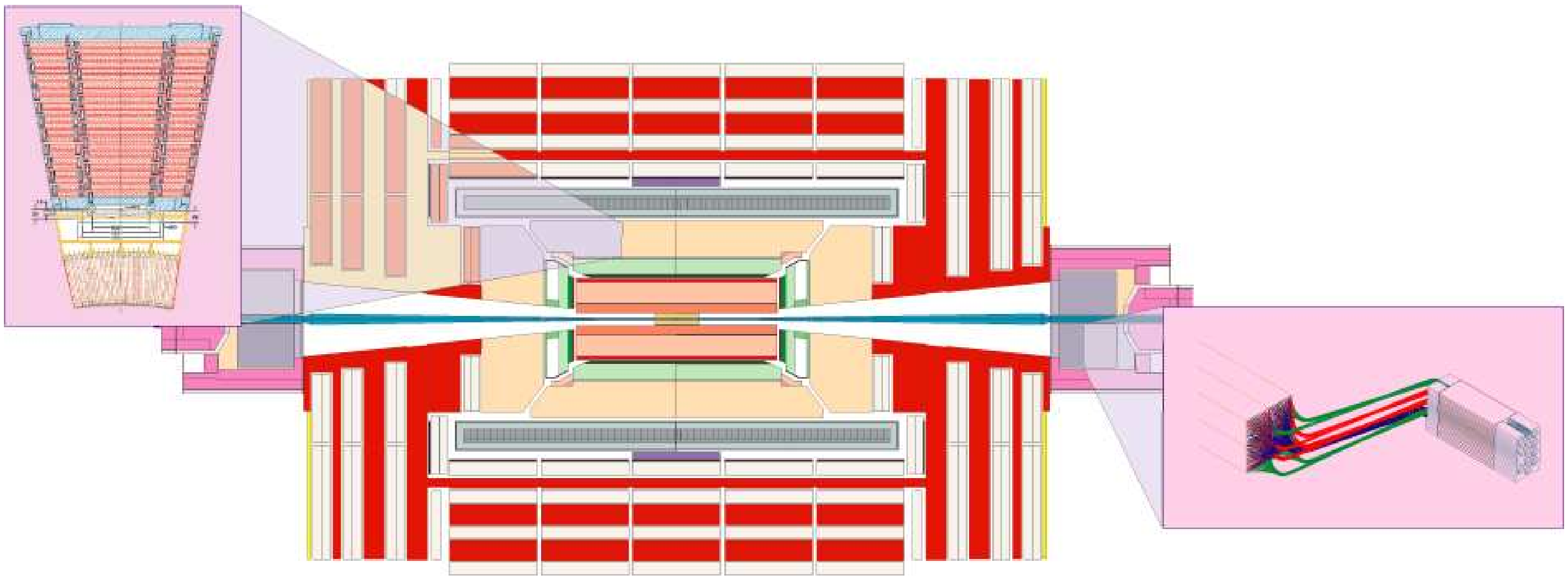

The Hadronic Calorimeter (HCAL), plays an essential role in the identification and measurement of quarks, gluons, and neutrinos by measuring the energy and direction of jets and of missing transverse energy flow in events.

The hadron barrel (HB) and hadron endcap (HE) calorimeters are sampling calorimeters with 50 mm thick copper absorber plates interleaved with 4 mm thick scintillator sheets.

There are two hadronic forward (HF) calorimeters, one located at each end of the CMS detector, which complete the HCAL coverage to $|\eta| = 5$.

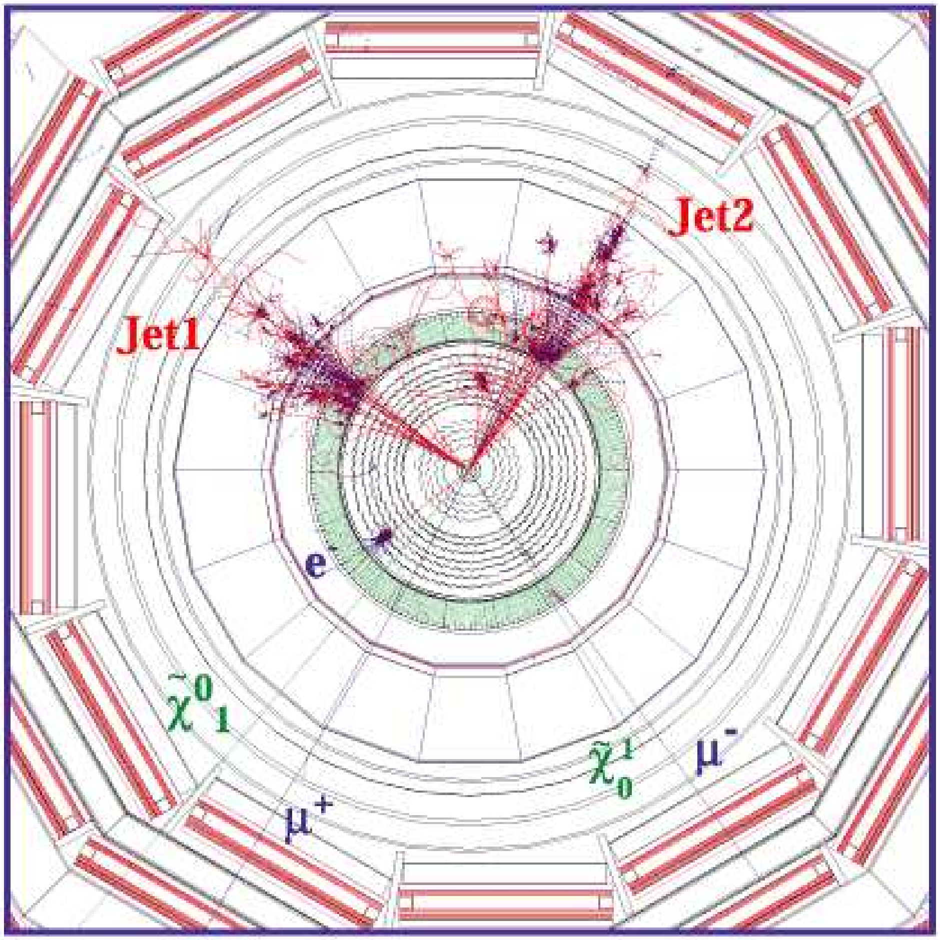

In this simulation jets are observed in the HB calorimeter. The hermeticity of the HCAL (the HB, HE and HF detectors working together) is used to identify the substantial missing energy in the event.

3.3 Muon Chamber

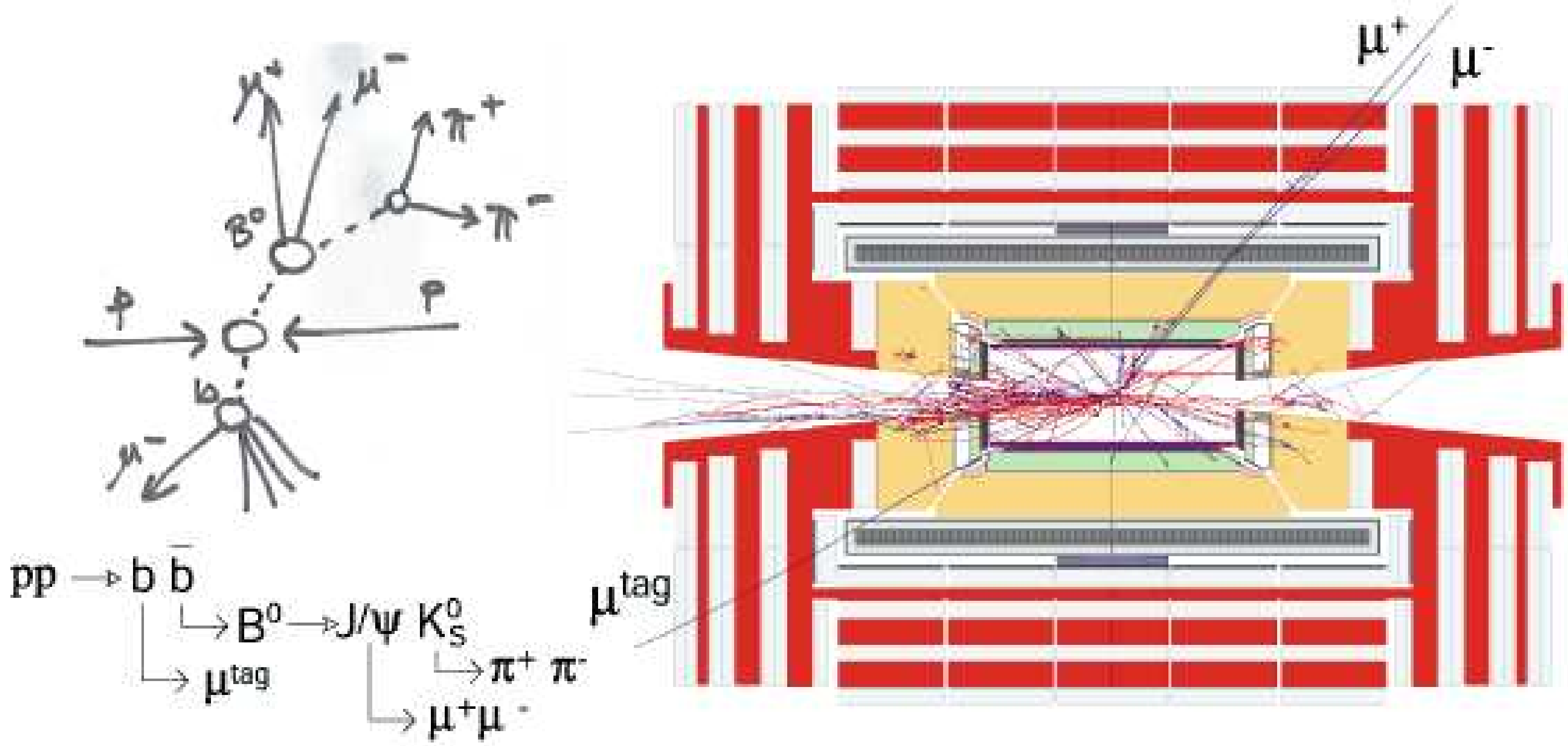

The muon detectors consist of four muon stations interleaved with the iron return yoke plates. They are arranged in concentric cylinders around the beam line in the barrel region, and in disks perpendicular to the beam line in the endcaps. They are shown in silver in the diagrams.

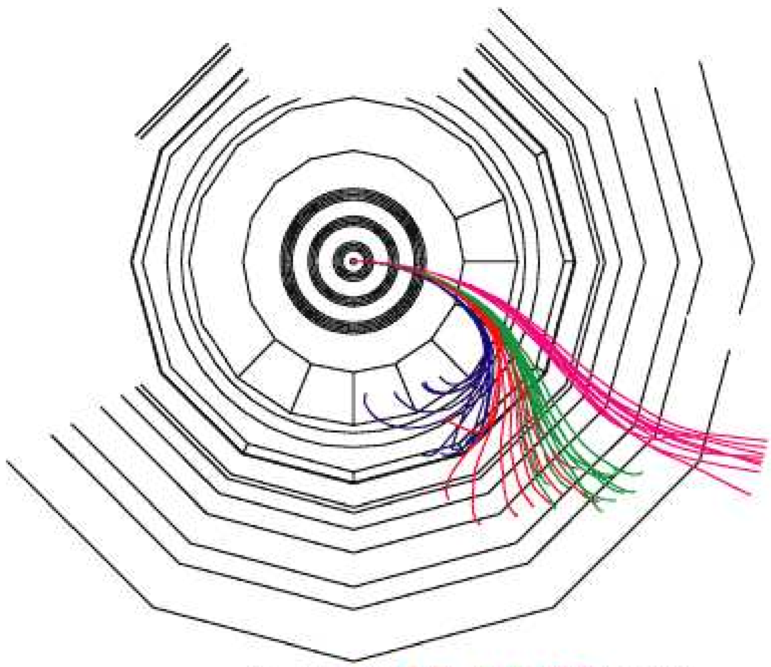

Muon identification is ensured by the large thickness of the absorber material (iron), which cannot be traversed by particles other than neutrinos and muons.

There are at least 10 interaction lengths (l) of calorimeters before the first station and an additional 10 l of iron yoke before the last station. The identification is achieved by lining-up the hits in at least two out of the four muon stations.

p_T can be measured down to a couple of GeV and up 7 TeV in the range $|\eta| < 2.4$.

4. A sample calculation at Hadron Collider: Drell-Yan

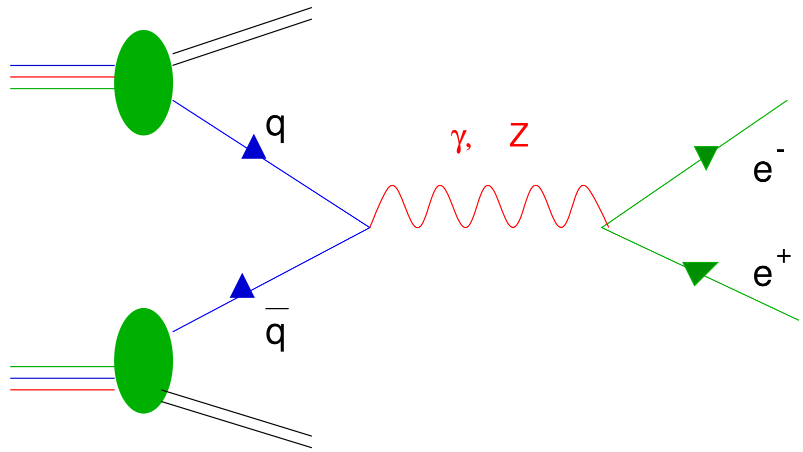

The final state lepton pair can probe the intermediate states to multi-TeV. DY is one of the best process to probe new resonances of many models, like RS gravitons, KK states of γ, Z, Z', ...

To calculate the production rates there are a few pieces putting together:

$$\sigma(pp \to \ell^+\ell^- + X) = \sum_{ij} \int \hat{\sigma}(ij \to X;\mu)\, f_{i/p}(x_1,\mu)\, f_{j/p}(x_1,\mu)\, dx_1 dx_2$$

where $f_{i/p}(x,\mu)$ is the parton distribution function of finding a parton i inside the proton with a momentum fraction x. $\hat{\sigma}$ is the subprocess cross section.

4.1 Calculate subprocess cross section

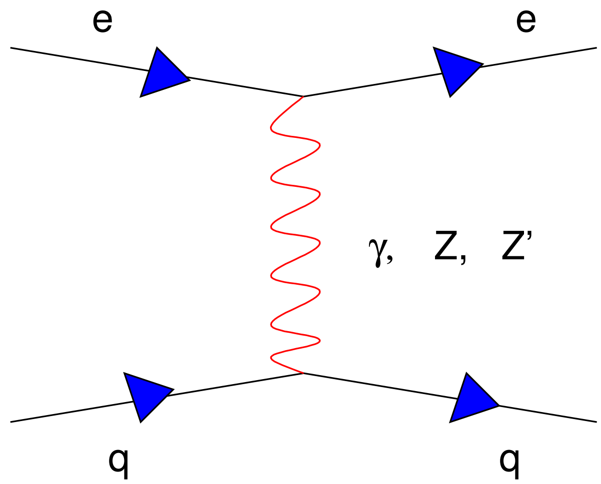

$$q\ (p_1)\quad \bar{q}\ (p_2) \to \ell^-\ (k_1)\quad \ell^+\ (k_2)$$

The NC (γ, Z, Z') interactions are given by

$$\mathcal{L}_{\rm NC} = -eJ^{\mu}_{\rm em}A_\mu - g_Z J^{(1)\,\mu} Z^0_{1\mu} - g_{Z'} J^{(2)\,\mu} Z^0_{2\mu}\ ,$$

where

$$J^{(2)}_\mu = \sum_{i,j} \overline{\psi}_i \gamma_\mu \left[\epsilon_{L_{ij}} P_L + \epsilon_{R_{ij}} P_R \right] \psi_j\ ,$$

- The amplitudes for the Feynman diagrams are

$$
\begin{aligned}
i\mathcal{M}_\gamma &= -ie^2 Q_q Q_\ell \, \frac{1}{s} \, \bar{v}(p_2)\gamma^\mu u(p_1) \; \bar{u}(k_1)\gamma_\mu v(k_2) \\
i\mathcal{M}_Z &= -i \frac{e^2}{\sin^2\theta_{\rm w}\cos^2\theta_{\rm w}} \, \frac{1}{s-m_Z^2} \, \bar{v}(p_2)\gamma^\mu \left(g_L^q P_L + g_R^q P_R \right) u(p_1) \\
&\quad \times \bar{u}(k_1)\gamma_\mu \left(g_L^\ell P_L + g_R^\ell P_R \right) v(k_2) \\
i\mathcal{M}_{Z'} &= -i g_{Z'}^2 \, \frac{1}{s-m_{Z'}^2} \, \bar{v}(p_2)\gamma^\mu \left(\epsilon_L^q P_L + \epsilon_R^q P_R \right) u(p_1) \\
&\quad \times \bar{u}(k_1)\gamma_\mu \left(\epsilon_L^\ell P_L + \epsilon_R^\ell P_R \right) v(k_2)
\end{aligned}
$$

- Square the terms, sum over initial and final helicities:

$$
\sum |\mathcal{M}|^2 = 4\hat{u}^2 \left(|M_{\rm LL}^{\ell q}|^2 + |M_{\rm RR}^{\ell q}|^2 \right) + 4\hat{t}^2 \left(|M_{\rm LR}^{\ell q}|^2 + |M_{\rm RL}^{\ell q}|^2 \right)
$$

where

$$
M_{\alpha\beta}^{\ell q} = \frac{e^2 Q_\ell Q_q}{\hat{s}} + \frac{e^2 g_\alpha^\ell g_\beta^q}{\sin^2\theta_W \cos^2\theta_{\rm w}} \, \frac{1}{\hat{s}-m_Z^2} + g_{Z'}^2 \epsilon_\alpha^\ell \epsilon_\beta^q \, \frac{1}{\hat{s}-m_{Z'}^2}
$$

Here $\hat{s}, \hat{t}, \hat{u}$ are the usual Mandelstam variables, $g_L^f = T_{3f} - Q_f \sin^2\theta_W$, $g_R^f = -Q_f \sin^2\theta_{\rm w}$, and Q_f is the electric charge of the fermion f in units of proton charge.

- Average initial state helicities and colors:

$$\overline{\sum}|\mathcal{M}|^2 = \frac{1}{4}\,\frac{1}{3}\sum|\mathcal{M}|^2$$

- Subprocess cross section:

$$d\hat{\sigma} = \frac{1}{(2\pi)^{(3n-4)}}\,\frac{1}{2\hat{s}}\,\overline{\sum}|\mathcal{M}|^2\, d(PS_2)$$

$$d(PS_2) = \delta^{(4)}(p_1+p_2-k_1-k_2)\,\frac{d^3k_1}{2k_1^0}\,\frac{d^3k_2}{2k_2^0} = \frac{\pi}{4}\,d\cos\theta^*$$

$$\frac{d\hat{\sigma}}{d\cos\theta^*} = \frac{1}{96\pi}\,\frac{1}{\hat{s}}\left[\hat{u}^2\left(|M_{\rm LL}^{\ell q}|^2+|M_{\rm RR}^{\ell q}|^2\right)+\hat{t}^2\left(|M_{\rm LR}^{\ell q}|^2+|M_{\rm RL}^{\ell q}|^2\right)\right]$$

$$\hat{\sigma} = \frac{\hat{s}}{144\pi}\,\left(|M_{\rm LL}^{\ell q}|^2+|M_{\rm RR}^{\ell q}|^2+|M_{\rm LR}^{\ell q}|^2+|M_{\rm RL}^{\ell q}|^2\right)$$

- Folded with parton distribution functions:

$$\sigma = \sum_q \int dx_1\, dx_2\, f_{q/p}(x_1)\, f_{\bar{q}/p}(x_2)\, \hat{\sigma}(\hat{s})$$

We can change the variables x_1 and x_2 to $M_{\ell\ell}$ and y:

$$\frac{d^2\sigma}{dM_{\ell\ell}dy} = K \frac{M_{\ell\ell}^3}{72\pi s} \sum_q f_{q/p}(x_1)\, f_{\bar{q}/p}(x_2)\, \left(|M_{\rm LL}^{\ell q}|^2 + |M_{\rm RR}^{\ell q}|^2 + |M_{\rm LR}^{\ell q}|^2 + |M_{\rm RL}^{\ell q}|^2 \right)$$

where

$$x_{1,2} = \frac{M_{\ell\ell}}{\sqrt{s}} e^{\pm y}, \quad K = 1 + \frac{\alpha_s}{2\pi} \frac{4}{3} \left(1 + \frac{4\pi^2}{3} \right)$$

$M_{\ell\ell} = \sqrt{(\ell_1 + \ell_2)^2}$ is the invariant mass of the lepton pair and y is the rapidity.

4.2 Parton Model

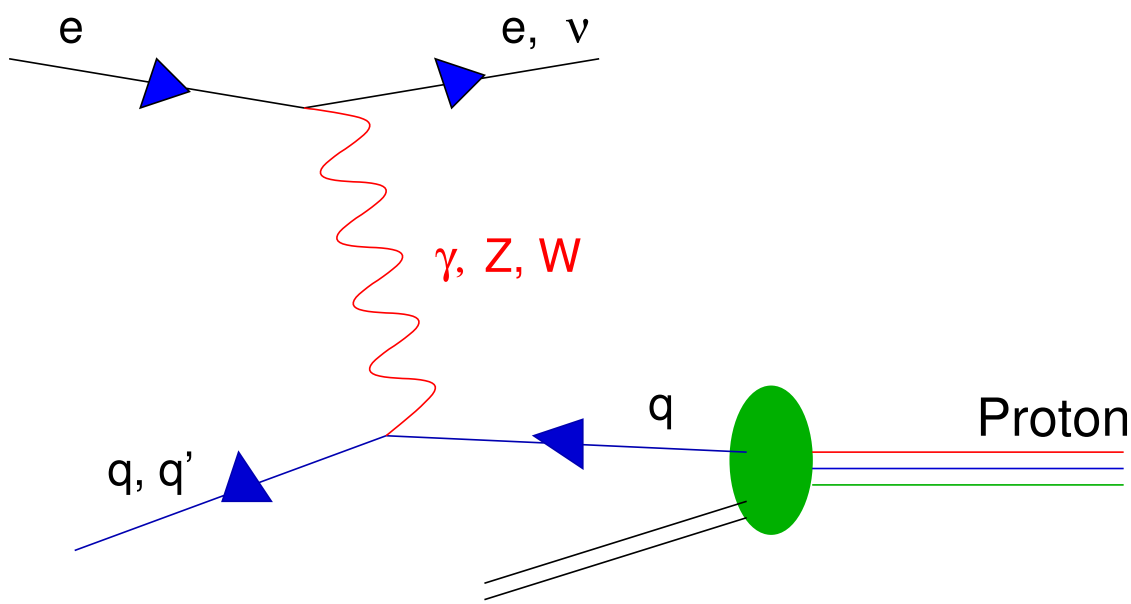

In typical e-N scattering experiment, the hadron state is unidentified. For deep-inelastic scattering (DIS) one measures E', θ and so Q^2, x, y:

$$Q^2 = -(p'_\ell - p_\ell)^2 \; = \; 2EE' \cos\theta, \quad x = \frac{Q^2}{2M_p \nu},$$

where $\nu = E'_\ell - E_\ell$ and y is a measure of the scattering angle:

$$y = \frac{Q^2}{\hat{s}} = \frac{Q^2}{sx}$$

The measured cross section can be expressed as

$$\frac{d\sigma}{dE' d\Omega'} = \frac{\alpha^2}{4E^2 \sin^4(\theta/2)} \frac{1}{\nu} \left[\cos^2(\theta/2) F_2(x, Q^2) + \sin^2(\theta/2) \frac{Q^2}{x M^2} F_1(x, Q^2) \right]$$

where F_1, F_2 are structure functions.

Bjorken Scaling: for fixed x the measured $F_1(x, Q^2)$ and $F_2(x, Q^2)$ are approximately independent of Q^2

$$F_{1,2}(x, Q^2) \simeq F_{1,2}(x) \quad \text{for} \;\; Q^2 \gg M_p^2$$

C.f. If proton is a point particle, its elastic form factor independent of Q^2. But strong Q^2 dependence for elastic form factor implies p is not a point particle.

The approximate scaling invariance in DIS was observed at SLAC in 1969

$\Rightarrow$ first dynamical evidence for point-like partons inside proton

Parton Model is put forward to interpret the approximate scale invariance. Parton is a point-like particle within the proton.

In the infinite momentum frame, the momentum of the parton is almost collinear with the proton. We can define the momentum fraction z as

$$z \equiv \frac{P_{\rm parton}}{P_{\rm proton}}$$

The measured cross section at a given $x \equiv Q^2/(2M\nu)$ is $\propto$ the probability of finding a parton with a momentum fraction z of the proton momentum:

$$z \equiv \frac{P_{\rm parton}}{P_{\rm proton}} = x \equiv Q^2/(2M\nu)$$

The structure function

$$F_2(x,Q^2) = \sum_a e_a^2 \, x \, f_a(x)$$

where $f_a(x)dx$ is the probability of finding a parton a of charge e_a with momentum fraction between x and $x + dx$.

The structure functions $F_{1,2}(x)$ show (Callan-Gross relation)

$$2xF_1(x,Q^2) = F_2(x,Q^2)$$

which decisively determined the spin-1/2 of the parton (quarks).

Parton Distribution Functions

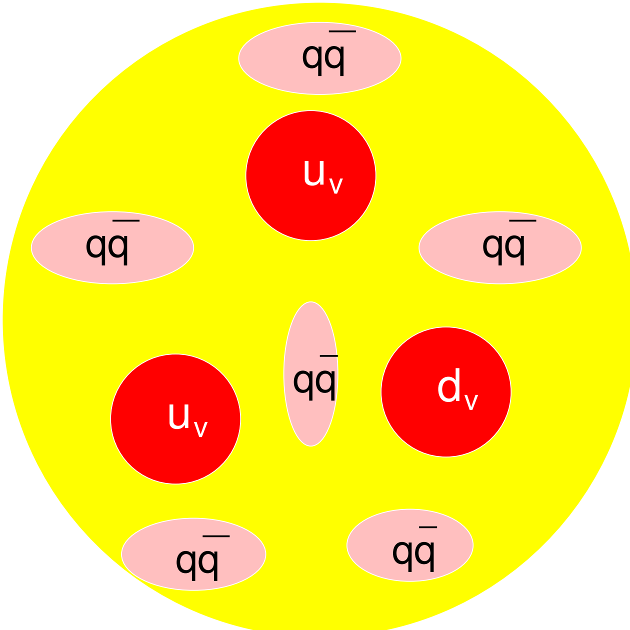

Valence and sea quarks

In e-N scattering, the lepton not only strikes the valence quarks but also the $q\bar{q}$ pairs of the sea. The parton distribution functions:

$$
\begin{aligned}
u(x) &= u_v(x) + u_s(x), \qquad \bar{u}(x) = u_s(x) \\
d(x) &= d_v(x) + d_s(x), \qquad \bar{d}(x) = d_s(x) \\
s(x) &= \bar{s}(x) = s_s(x) \\
c(x) &= \bar{c}(x) = c_s(x) \\
b(x) &= \bar{b}(x) = b_s(x)
\end{aligned}
$$

CTEQ6M

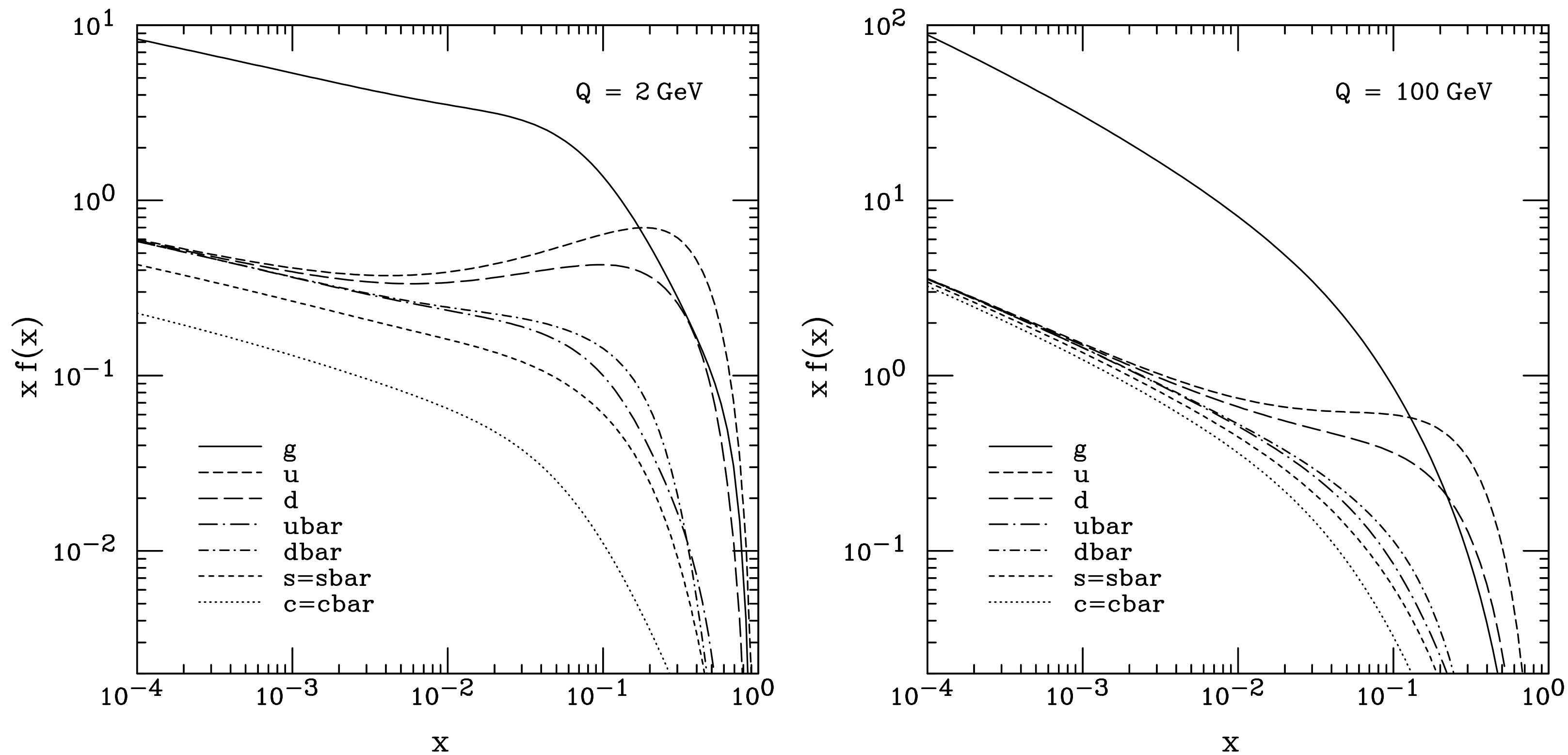
Q = 2 GeV
Q = 100 GeV
x f(x)
x
g
u
d
ubar
dbar
s=sbar
c=cbar
10^{1}
10^{0}
10^{-1}
10^{-2}
10^{2}
10^{-4}
10^{-3}

Putting PDF and $\hat{\sigma}$ together

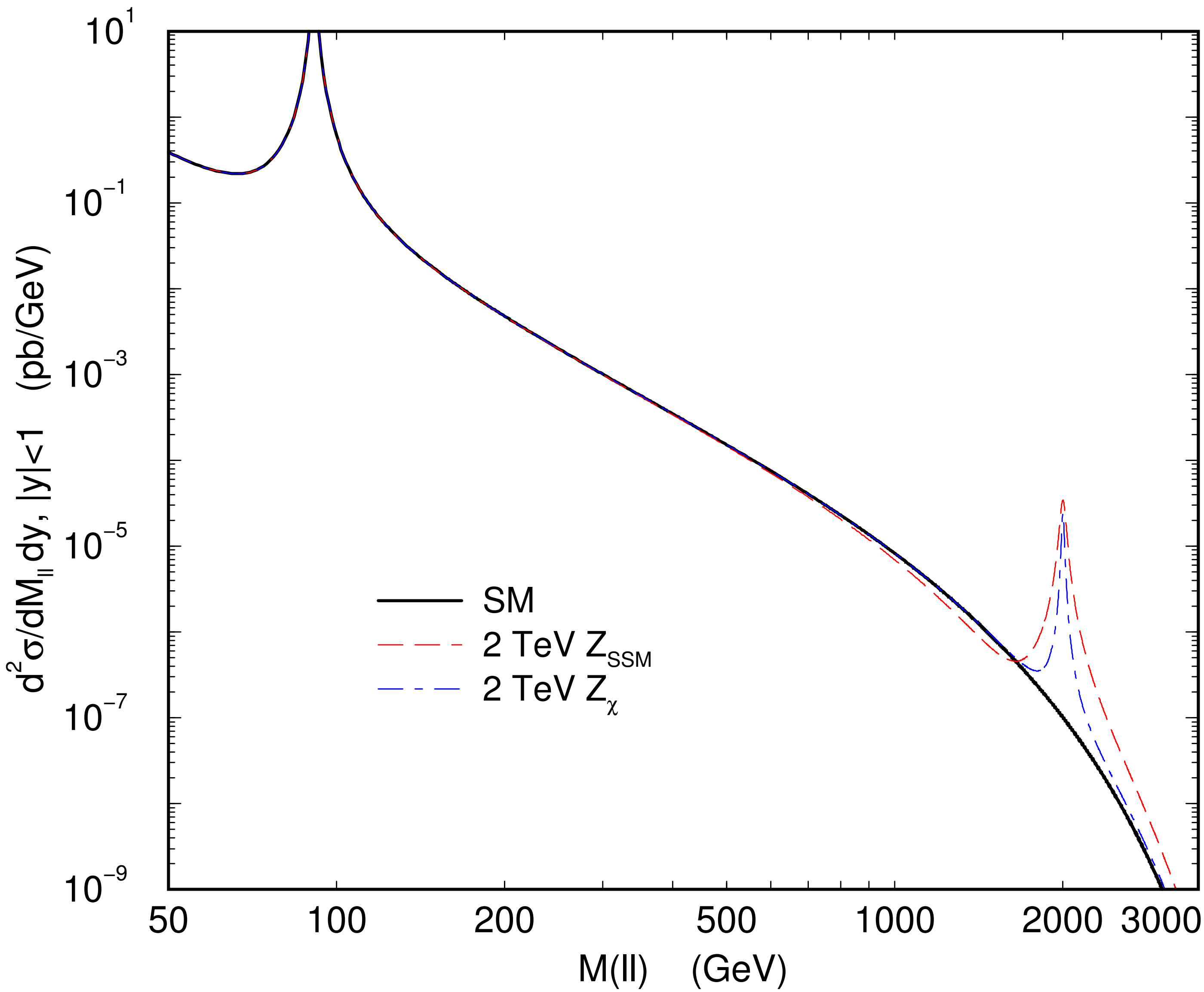

5. Kinematics

We need to use some kinematic variables to identify the dynamics of the signal. In the previous example, the most obvious kiematic variable is the invariant mass of the lepton pair $M_{\ell\ell}$. It signifies the presence of the Z'

Different processes may require different kinematic variables to identify the dynamics.

Here are some basic kinematic variables to consider. In a pp collision like the LHC, the actual collision can be thought as colliding a parton with momentum $p_1 = x_1 P_A$ with another parton with momentum $p_2 = x_2 P_B$:

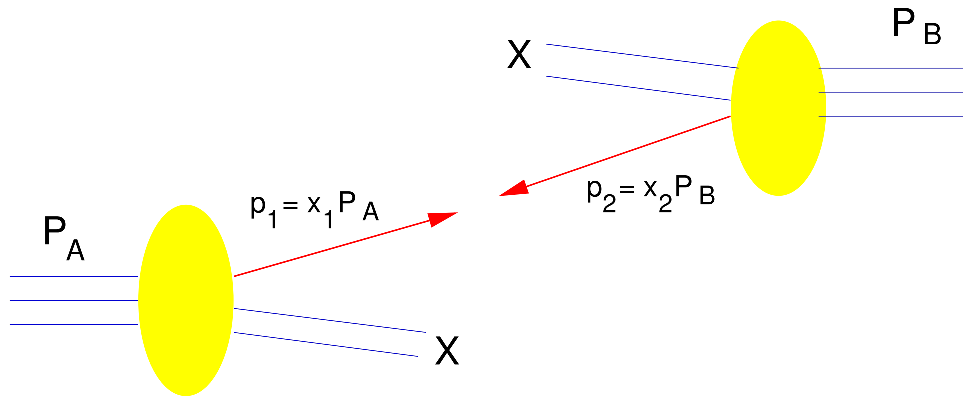

In pp collision, suppose

$$P_A = \left(\frac{\sqrt{s}}{2}, 0, 0, \frac{\sqrt{s}}{2}\right) \qquad P_B = \left(\frac{\sqrt{s}}{2}, 0, 0, -\frac{\sqrt{s}}{2}\right)$$

$$p_1 = \left(x_1\frac{\sqrt{s}}{2}, 0, 0, x_1\frac{\sqrt{s}}{2}\right), \qquad p_2 = \left(x_2\frac{\sqrt{s}}{2}, 0, 0, -x_2\frac{\sqrt{s}}{2}\right)$$

The parton CM frame is moving with

$$P_{\rm cm} = \left((x_1+x_2)\frac{\sqrt{s}}{2}, 0, 0, (x_1-x_2)\frac{\sqrt{s}}{2}\right)$$

and the rapidity $y_{\rm cm}$ of the parton CM frame is

$$y_{\rm cm} = \frac{1}{2}\,\ln\frac{x_1}{x_2}$$

We can express x_1 and x_2 as

$$x_{1,2} = \sqrt{\hat{s}/s}\; e^{\pm y_{\rm cm}}$$

where $\hat{s} = x_1 x_2 s$ is the CM energy-square of the partons.

Other useful variables are

- Transverse momentum $p_T = p\sin\theta$. The momentum in the direction $\perp$ beam-pipe. It is impossible to measure particles going down the beam-pipe. Also transverse momentum is invariant under longitudinal boost.

- Rapidity:

$$y = \frac{1}{2} \ln \frac{E + p_z}{E - p_z}$$

If the parton frame is boosted along the longitudinal direction, the new rapidity is given by

$$y' = \frac{1}{2} \ln \frac{E' + p'_z}{E' - p'_z} = \frac{1}{2} \ln \frac{(1 - \beta_0)(E' + p'_z)}{(1 + \beta_0)(E' - p'_z)} = y - y_0$$

Therefore, the difference in rapidities is invariant under a longitudinal boost

$$\Delta y' = y'_2 - y'_1 = (y_2 - y_0) - (y_1 - y_0) = y_2 - y_1 = \Delta y$$

In the massless limit

$$y = \frac{1}{2} \ln \frac{1 + \cos\theta}{1 - \cos\theta} = \ln \cot \frac{\theta}{2} \equiv \eta$$

- Separation in (θ, ϕ) plane:

$$\Delta R = \sqrt{(\Delta\eta)^2 + (\Delta\phi)^2}$$

The concept of ΔR is used to define a jet cone.

- Invariant mass of a system of particles: $\sqrt{(p_1 + p_2 + \ldots)^2}$. It is very useful to test if the set of particles is the decay products of a single species. For a Z' $M_{\ell\ell}$ shows a peak at $M_{Z'}$.

- Missing transverse momentum: (i sums over all visible particles)

$$\not{p}_T = -\sum_i p_{T_i}$$

It is important if the final state consists of ν, $\widetilde{\chi}_1^0$, gravitons, ...

- Transverse mass: for example in the decay $W \to e\nu$, the neutrino is missing. So only the missing transverse momentum can be measured. We define the transverse mass as

$$M_T^2 = (E_{eT} + \not{E}_T)^2 - (\vec{p}_{eT} + \vec{\not{p}}_T)^2$$

It can show the partial structure of the resonance.

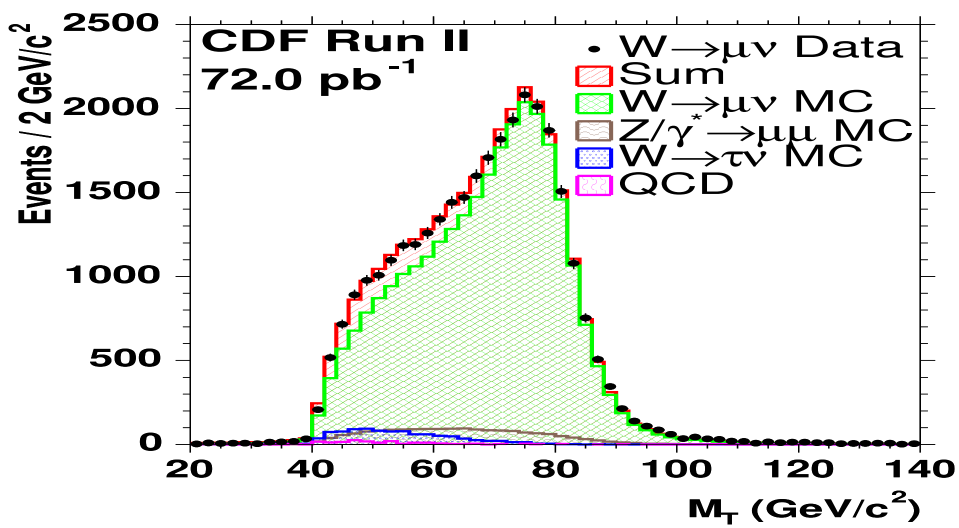

5.1 Kinematic variables used in heavy $H \to ZZ$ search

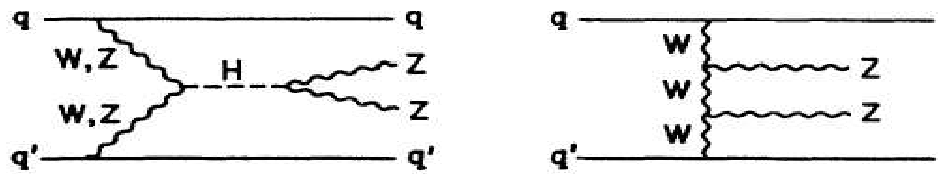

(a)

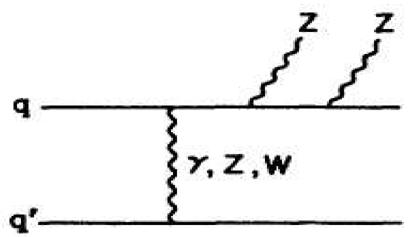

(b)

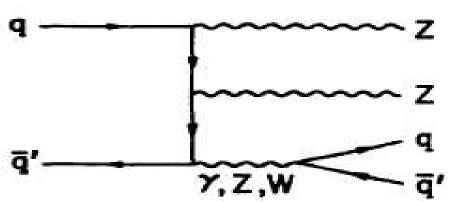

(c)

To enhance the heavy Higgs effect and to reduce backgrounds.

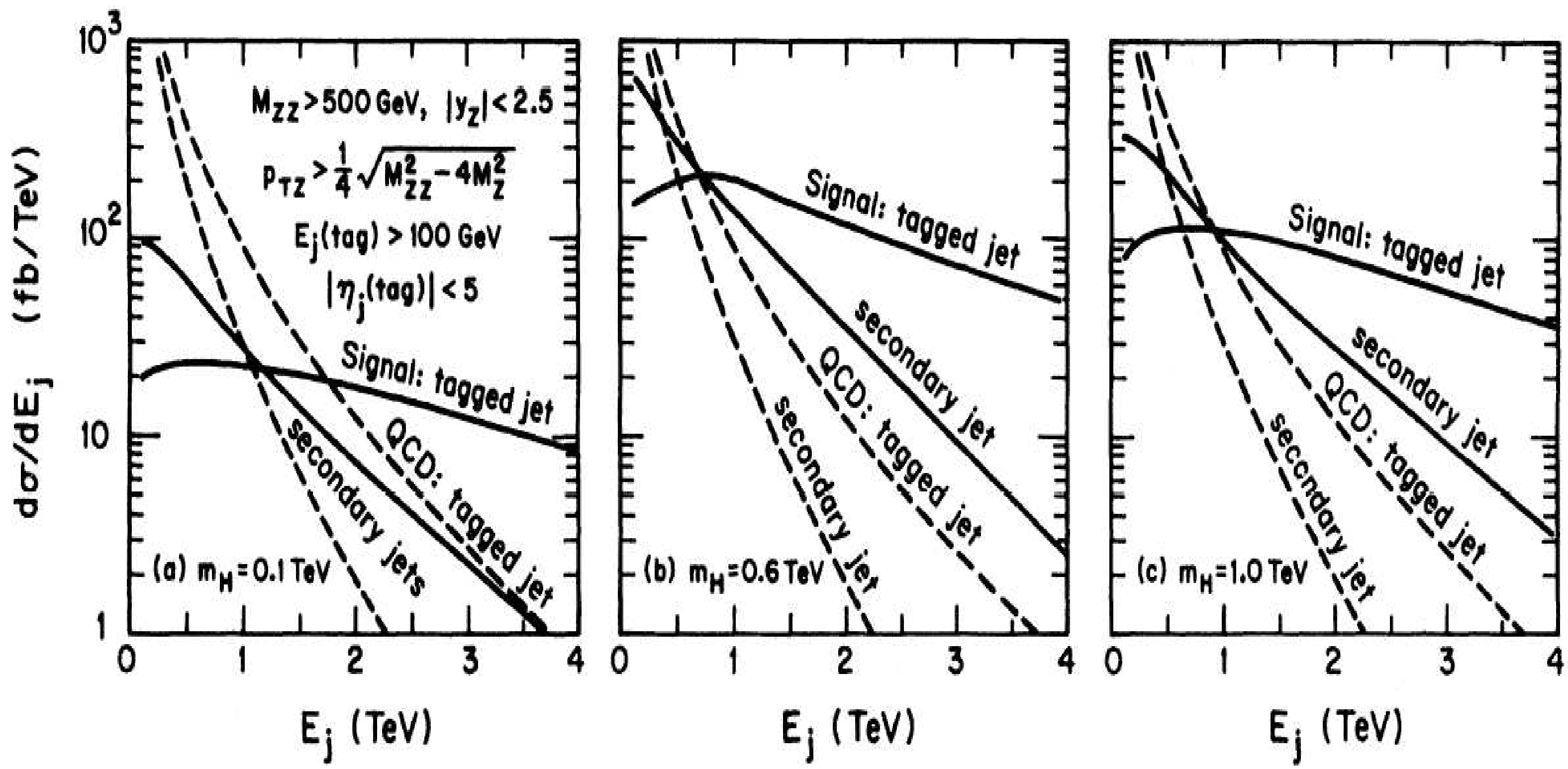

A forward energetic jet

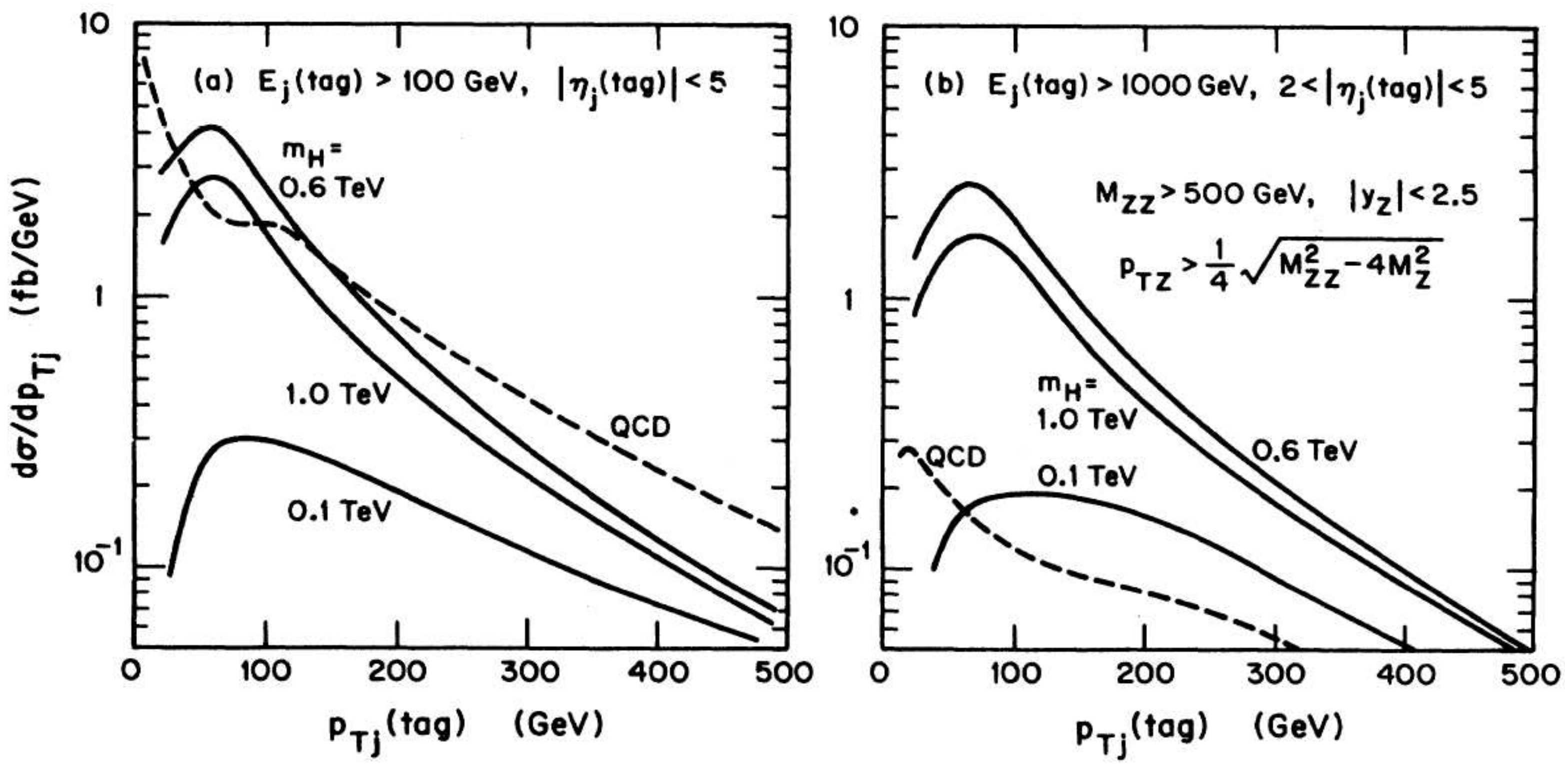

The transverse momentum is not so useful

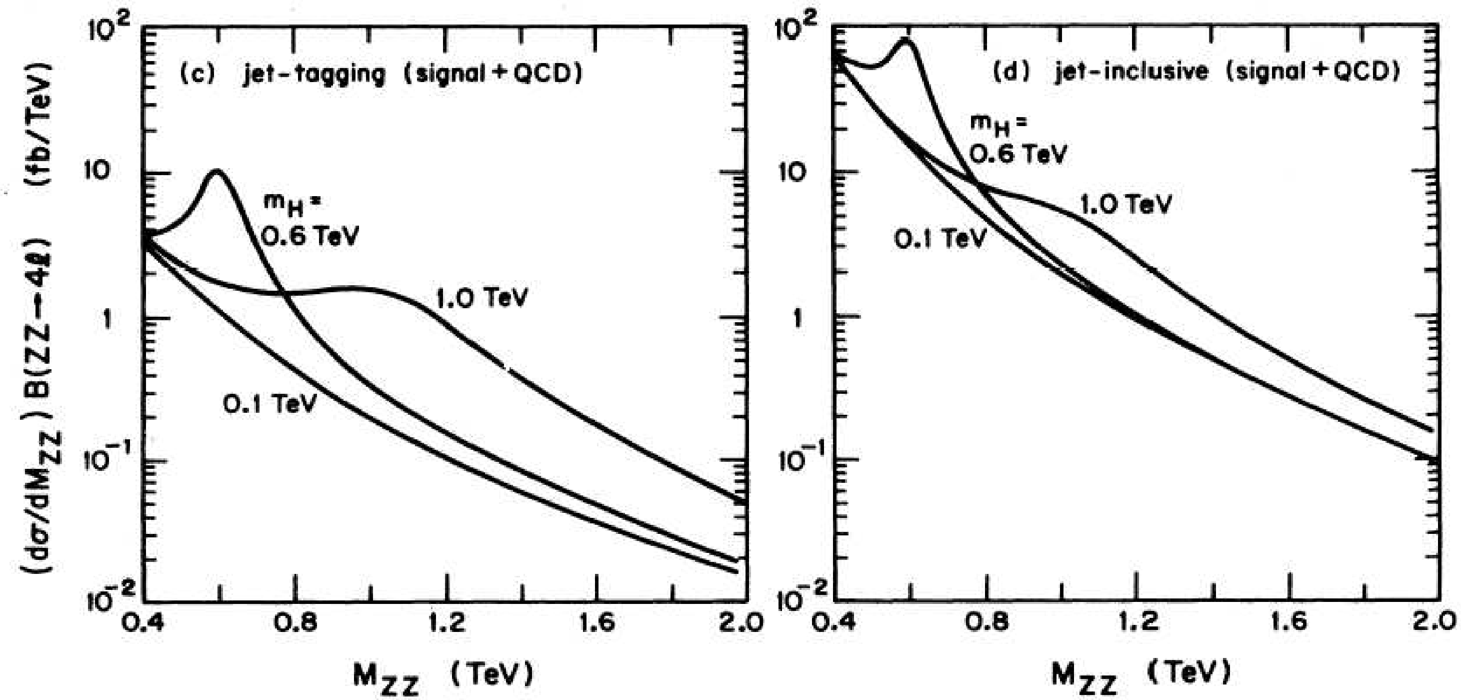

The invariant mass spectrum shows a clear resonace structure

5.2 Monte Carlo (MC) Approach to handle event selections

Experimental event selections often impose various cuts to enhance the signal-to-background ratio. It is important to simulate the experimental cuts in evaluating the cross sections. Monte carlo approach is useful in this respect.

In general, one can do parton-level event simulations. If you can beat the background, then you can tell the experimenters to do a full simulation.

Tools: a good adaptive monte carlo integration routine, e.g., VEGAS.

- it contains a random-number generator
- an adaptive integration algorithm to sample the more relevant phase space

Using MC approach, one can easily impose complicated sets of cuts to enhance the signal-to-background ratio.

An example: $pp \to (\tilde{g}\tilde{g}) \to t\bar{t}$

A heavy resonance (gluinonium) decaying into $t\bar{t}$ to be against the SM $t\bar{t}$ background.

Selection cuts:

1. A large transverse momentum p_T on the t and $\bar{t}$

$$p_T > \frac{3}{8} M$$

2. Require the t and $\bar{t}$ in the central rapidity region

$$|y| < 2$$

3. Require the invariant mass $M_{t\bar{t}}$ in a mass window of M

$$|M_{t\bar{t}} - M| < 50 \text{ GeV}$$

We can impose the cuts simultaneously on the signal and background.

Signal-to-background ratio and Significance

S/B is important but sometimes the significance is more relevant

$$\text{Significance} = \frac{S}{\sqrt{B}}$$

Here S is the number of the signal events, B is the background events.

If one can calculate the B with high precision, then $\sqrt{B}$ is the standard deviation, and $S/\sqrt{B}$ is the number of significance.

Say, the $S/B = 1/2$. If we double the luminosity, the S/B is the same, but

$$\frac{S}{\sqrt{B}} \text{ increases by } \sqrt{2}$$

That is why luminosity of the LHC is important.